Ninth International Conference on
THIN-WALLED STRUCTURES – ICTWS2023
Sydney, Australia, Nov 29 – Dec 1, 2023

PROGRESSIVE COLLAPSE OF BEAM-TO-UPRIGHT SUBASSEMBLIES OF STEEL STORAGE RACKS UNDER A COLUMN REMOVAL SCENARIO

Liusi Dai[1], Hao Yao[1], Chong Ren[1,*]

1. School of Civil Engineering, Shanghai University, Shanghai, China.
* Corresponding author, Email: chongren@shu.edu.cn

Keywords: Steel storage racks; Progressive collapse; Experiments; Connection detailing.

Abstract. *This paper presents an experimental investigation into progressive collapse behaviour of steel storage pallet racks under a column removal scenario. The double-half-span substructure is applied in experimental tests. A total of eight substructures are tested, considering two types of beam-to-upright connections, i.e., boltless and bolted connections, commonly used in pallet racks. Different upright profiles and thicknesses, varied beam heights, and the number of tabs are carefully considered in the tests, and their effects on progressive collapse behaviour of pallet racks are thus evaluated. In particular, the influence of pallet loads is carefully evaluated in this paper. Detailed experimental results of all specimens are provided, including the full-range load-displacement curves and the failure modes. The dominated failure modes observed in the tests are tab crack (T), the combination of tab crack and bolt bearing failure leading to tearing of beam-end-connector (T+B), and the combination of tab crack and bolt bearing failure leading to tearing of upright wall (T+C). The test results revealed that the presence of pallet loads greatly influences structural progressive collapse behaviour and thus should be considered in further studies. Moreover, in bolted connections, smaller beam heights and thinner column thicknesses exhibit better resistance against progressive collapse. Whereas in boltless connections, increasing the number of tabs enhances the resistance against progressive collapse. Generally, bolted connections are proven to have better resistance against progressive collapse than boltless connections, and can be used in storage racks to improve the structural robustness.*

1 INTRODUCTION

In recent years, there has been a continuous increase in incidents of building progressive collapse worldwide. Therefore, an increasing number of researchers and engineers are paying attention to structural progressive collapse and conducting relevant studies. The definition of progressive collapse is that "Progressive collapse refers to some scenario where local initial damage in a structure propagates to other elements under accidental loads, resulting in a disproportionate collapse of structural parts or the entire structure [1]". Since steel storage racks are composed of cold-formed thin-walled steel members connected by mechanical connections and with the development of logistic industry racks can be as high as 30-50 meters, more and more progressive collapse accidents caused by unintentional impacts are reported. However, limited researches have been conducted on progressive collapse of rack structures.

Generally, bracing members are not arranged in the down-aisle direction of cold-formed thin-walled steel pallet racks, and thus the behaviour semi-rigid and partial strength beam-to-upright connections are of great importance for providing the lateral resistance. Some researchers [2-5] conducted static and hysteretic tests on boltless and bolted connections commonly used in pallet racks, obtaining the typical failure modes, initial stiffness, moment capacity, and energy dissipation capacity. Based on this, Zhao et al. [6] proposed a theoretical model for boltless beam-to-upright connections that aligns with the experimental results. The

results indicated that the initial stiffness and moment capacity of bolted connections were superior to boltless connections. However, these studies are limited to the static and seismic behaviour of racks. As for the dynamic behaviour of racks [7-9] under forklift impact, Ng et al. [7] investigated the dynamic response of assembled racking structures under a single leg removed by impact and the overall structural response after the failure of the upright base-plate, proposing strengthening strategies for the support system and column base connections to enhance the structural resistance against progressive collapse. B.P. Gilbert et al. [8, 9] conducted a systematic study on a forklift-impacted drive-in rack, using full-scale static and dynamic tests to develop simplified analytical models of loaded forklifts and a drive-in rack through refined finite element analysis.

However, there is still a lack of in-depth research on progressive collapse of rack structures. The methodology of double-half span substructure is widely accepted for progressive collapse studies of frame structures and is applied in research on pallet racks, particularly for the down-aisle directions. This paper investigates the performance of steel rack beam-to-upright subassemblies under the column removal scenario, and the double-half span substructures with steel storage pallet rack boltless and bolted connections are considered. Eight test specimens considering different connection details variables were tested, and typical failure modes and the progressive collapse-resisting mechanisms were identified. Finally, recommendations to enhance the resistance of steel storage pallet racks to progressive collapse are provided.

2 TEST SPECIMENS AND SETUP

2.1 Test specimens

As depicted in Figure 1 an Figure 2, this study focuses on the progressive collapse behaviour of double-half-span substructures of beam-to-upright connections in a cold-formed thin-walled steel storage pallet rack under a column removal scenario.

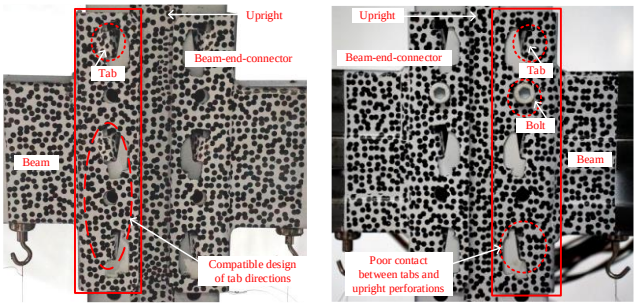

(a) Boltless connection (b) Bolted connection

Figure 1: Typical beam-to-upright boltless and bolted connections.

In accordance with [10], a typical steel storage pallet rack with a 2400mm span is selected, and two types of beam-to-upright connections, i.e., boltless and bolted connections (Figure 1), are considered. The test specimen for a double-half-span substructure comprises two beams, a vertical column, and two beam-end-connectors. These components are interconnected using four-sided fillet welds, joining the beam to the beam-end-connector. Note that the distance from the hinge support center to the beam end is 200 mm, and the distance between the two beam-end-connectors on both sides is 109 mm. Thus, the length of the beam is taken as 946 mm, and the length of the column is defined as 770 mm. In addition, the thickness of the beam-end-connector is 3.25mm, and the total length of the beam-to-upright connections substructure test specimen is 2400mm.

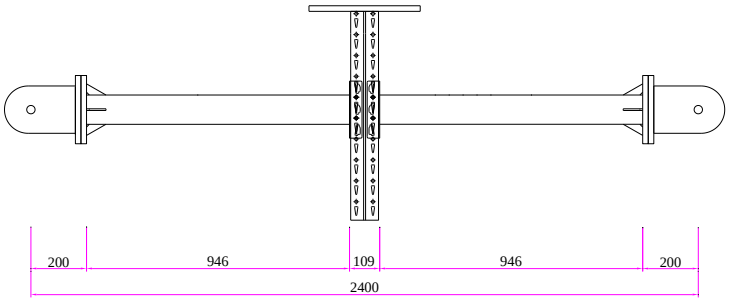

Figure 2: Geometry of test specimens.

Table 1: Specimen details.

Specimen	Beam-end-connector type	Column thickness (mm)	Beam height (mm)	Number of tabs	Number of bolts	Weight of load (kg)	Variation
2.5C-B105-2T-2400-L500	Boltless	2.5	105	2	0	500	Tabs
2.5C-B105-3T-2400-L500	Boltless	2.5	105	3	0	500	Type of connection
2.5C-B105-3TB-2400-L500	Bolted	2.5	105	3	1	500	Height of beam
2.5C-B120-3TB-2400-L500	Bolted	2.5	120	3	1	500	
2.5C-B160-3TB-2400-L500	Bolted	2.5	160	3	1	500	
2.0C-B120-3TB-2400-L500	Bolted	2.0	120	3	1	500	Thickness of upright
3.0C-B120-3TB-2400-L500	Bolted	3.0	120	3	1	500	
2.5C-B120-3TB-2400-L0	Bolted	2.5	120	3	1	0	Weight of load

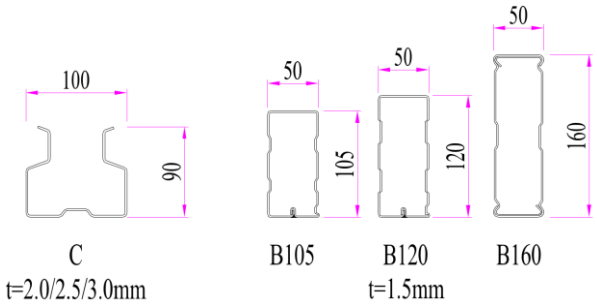

Figure 3: Section of column and pallet beams.

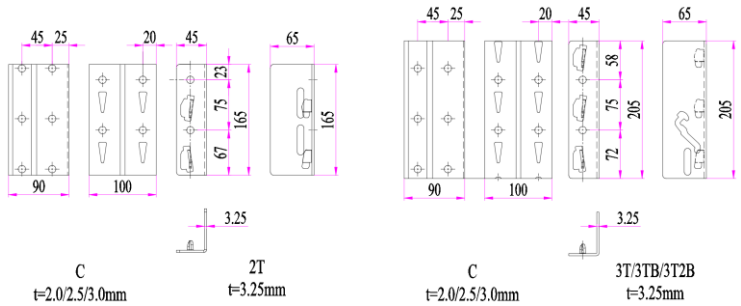

Figure 4: Typical perforations in column webs as well as flanges and the corresponding beam-end-connectors.

As illustrated in Table 1, a total of eight specimens are tested taking the main influential parameters, i.e., beam-end-connector type, beam height, column thickness, number of tabs, number of bolts, and with or without pallet loads, into consideration. Figure 3 displays the cross-sectional views of both columns and beams, providing valuable geometric insights. Figure 4 presents a clear illustration of the specific construction of various beam-end-connector types, featuring bolt holes with a diameter of 11mm, slightly larger (by 1mm) than that of the bolts

used. During the installation process, the bolts were tightened using a wrench, following the established procedure for assembling steel storage pallet racks. This ensured a secure and snug fit between the column and the beam-end-connectors.

2.2 Test setup and loading protocol

Figure 5 (a) depicts the experimental setup for the beam-to-upright connection substructure. The specimens are horizontally supported at both ends via hinge connections to triangular reaction brackets, ensuring lateral stability. Vertical loads are applied using an electric hydraulic servo actuator on a loading column, which is supported by a reaction frame. Both the triangular reaction brackets and reaction frame are firmly anchored to the ground, ensuring sufficient stiffness and resistance to potential loads and deformations. In order to enable free vertical movement of the column during the test, a vertical restraint sliding device is employed to provide vertical constraint to the loading column. This mechanism allows the column to move vertically and restrain the possible lateral displacements during the whole loading process.

For specimens with the presence of pallet loads, the loading procedure involves two schemes. For specimens with pallet loads, a specialized loading device (depicted in Figure 5 (b)) is used to apply pallet loads on the steel rack beams, simulating real-world scenarios. The pallet loads are applied at three levels on each side: 66kg, 84kg, and 100kg, each level being sustained for 2 minutes. After exerting the pallet loads, the load is applied on the column of specimens, and controlled by displacements. The displacement is carried out in three levels: the first level applies a loading rate of 1mm/min to achieve a 10mm displacement, the second level uses a loading rate of 3mm/min to achieve a 30mm displacement, and the third level utilizes a loading rate of 5mm/min until the completion of the test. For specimens without pallet loads, it is subjected to the vertical displacement loading scheme on the columns.

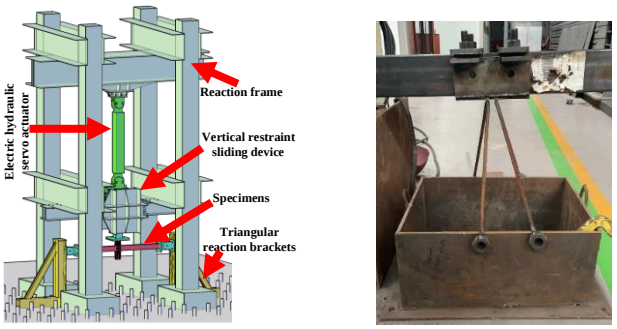

(a) Test setup (b) Facilities of assistant in applying loads

Figure 5: Test setup and facilities of assistant in applying loads.

2.3 Instrumentation

Figure 6 shows all measurement devices used in the experiment. Eight displacement transducers (D1-D8) are placed on the bottom flange of the beams to measure specimen vertical displacement during the test. One displacement transducer (D13) is positioned on the back surface of the column web to gauge vertical displacement at the midpoint of the column. Additionally, four displacement transducers (D9-D12) are installed at the hinge supports to monitor potential displacements during the test. Each test involved 32 strain gauges for measurements, strategically placed along the length of each beam at two cross-sections of each beam (L1 and L2 or R1 and R2). Each selected cross-section of each beam was equipped with eight strain gauges to measure the internal forces within the beam at that specific section. These

measurements were utilized to calculate the vertical resistance of specimens, as depicted in Figure 6.

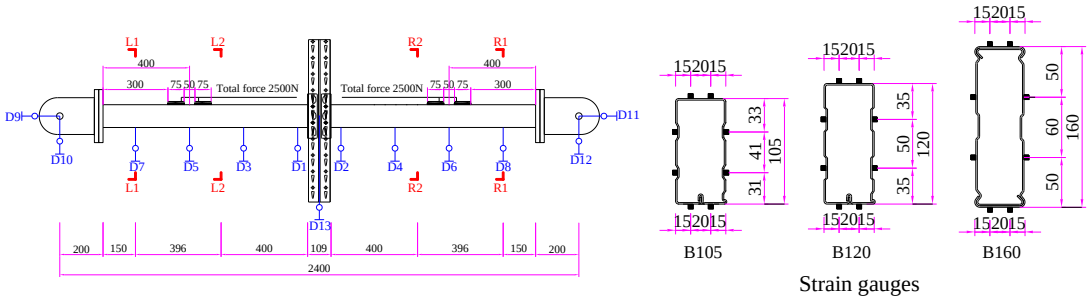

Figure 6: Experimental instrumentation arrangement.

3 TEST RESULTS

3.1 General

This section presents the test results with emphasis on an assessment of the resistance mechanism and load transfer path from the flexural stage to the catenary stage in the progressive collapse of the beam-to-upright subassemblies under the central column removal scenario. Internal force components at different response stages are investigated during the whole test.

Following the methodology proposed by [11], strain measurements were obtained at Sections L1 and R1, away from the connection regions of beam-to-upright subassemblies. Throughout the entire experimental process of central column removal, all recorded strains at this interface remained below the initial yielding strain of the material, indicating the cross-sections exhibit elastic behavior. Consequently, these strains measurement can be employed for calculating the internal forces of the Section L1 or R1 of the beams.

At Sections L1 and R1, the cross-sections are assumed to remain plane under combined bending and axial tension. As a result, the axial force N and the bending moment M can be determined using equations Eqs. (1) and (2), respectively.

$$N = EA \bullet \bar{\varepsilon} \tag{1}$$

$$M = EI \bullet \frac{\varepsilon_U - \varepsilon_L}{H} \tag{2}$$

where E is the elastic modulus; A is the cross-sectional area of the beam; I denotes the second moment of area of the cross-section of the beam; ε_U and ε_L correspond to the average axial strains of the top and bottom flanges, respectively, are determined by averaging all measured strains on the respective surfaces of the cross-section of the beam; $\bar{\varepsilon}$ is the axial strain of the section, which can be calculated by averaging the strains measured at evenly and symmetrically spaced locations along the height of the beam. H represents the height of the beam.

Based on the data recorded by displacement transducers placed along the length of the beam, it is observed that the beam maintains a predominantly straight configuration throughout the entire loading process. This finding aligns with the outcomes of other experimental investigations on substructures under the central column removal scenario [11, 12]. Consequently, the shear force at Sections L1 or R1 of the beam can be calculated using the force equilibrium, as indicated in Eq. (3).

$$V = \frac{M}{\sqrt{l^2 + \delta^2}} \tag{3}$$

where l is the distance from the hinge support to the Section at L1 or R1, and δ represents the vertical deformation of the section.

The vertical resistance of the specimen is composed of the flexural action (F_f) and the catenary action (F_c), which are calculated using Eq. (4) and Eq. (5), respectively.

$$F_f = V_{L1}\cos\theta_{L1} + V_{R1}\cos\theta_{R1} \tag{4}$$

$$F_c = N_{L1}\sin\theta_{L1} + N_{R1}\sin\theta_{R1} \tag{5}$$

where V_{L1}, N_{L1}, and θ_{L1} are the shear force, axial force, and rotation angle of Section L1, respectively. Similarly, V_{R1}, N_{R1}, and θ_{R1} represent the shear force, axial force, and rotation angle of Section R1, respectively. The rotation of a section angle, θ, is computed using Eq. 6.

$$\theta = \tan^{-1}(\delta / l) \tag{6}$$

Finally, the total vertical resistance of the specimen is provided by F, which is a combination of F_f and F_c, as shown in Eq. 7.

$$F = F_f + F_c \tag{7}$$

3.2 Load-displacement response and failure modes

The load-displacement curves of the specimens were analyzed, and the vertical force was determined using the total vertical resistance F from Eq. 6 and the vertical displacement measured by the D13 displacement transducer at the midpoint of the column, as detailed in Section 2.3. As illustrated in Figure 7, the eight specimens under the central column removal scenario exhibited three distinct failure modes: the dominated failure modes observed in the tests are tab crack (T), the combination of tab crack and bolt bearing failure leading to tearing of beam-end-connector (T+B), and the combination of tab crack and bolt bearing failure leading to tearing of column wall (T+C).

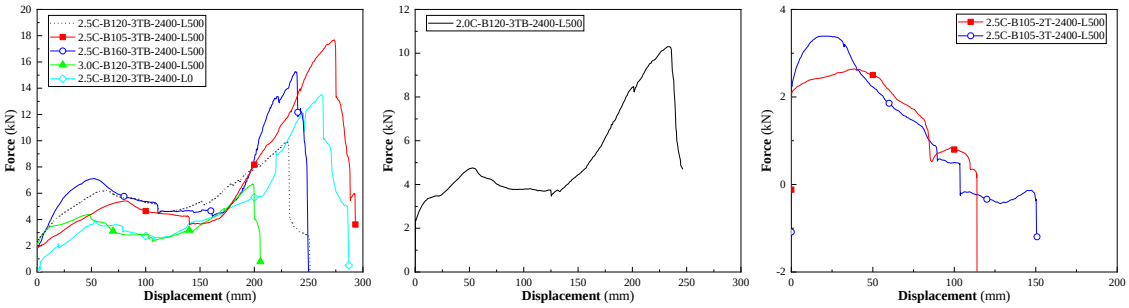

(a) T+B (b) T+C (c) T

Figure 7: Experimental load-displacement response of different failure modes.

The failure modes and corresponding experimental results of each specimen are summarized in Table 2. Figure 8 (a) presents the load-displacement curve for Specimen 2.5C-B120-3TB-2400-L500, highlighting critical stages during the test. The failure mode of specimen 2.5C-B120-3TB-2400-L500 is categorized as the combination of tab crack and bolt bearing failure leading to tearing of beam-end-connector (T+B). In Figure 8 (b), both the tabs and the top bolt

hole of the left beam-end-connector have fractured, and slight deformations are observed at the corresponding holes and bolt positions on the column.

Table 2: Summary of experimental results and failure modes of connection.

Specimen	Failure mode[#]	First peak		Ultimate	
		Resistance (kN)	Displacement (mm)	Resistance (kN)	Displacement (mm)
2.5C-B105-2T-2400-L500	T	2.64	38.6	2.64	38.6
2.5C-B105-3T-2400-L500	T	3.39	19.3	3.39	19.3
2.5C-B105-3TB-2400-L500	T+B	5.41	80.7	17.68	273.8
2.5C-B120-3TB-2400-L500	T+B	6.21	62.8	9.89	230.3
2.5C-B160-3TB-2400-L500	T+B	7.12	52.6	15.27	237.7
2.0C-B120-3TB-2400-L500	T+C	4.76	52.8	10.3	237.7
3.0C-B120-3TB-2400-L500	T+B	4.38	47.8	6.71	198.3
2.5C-B120-3TB-2400-L0	T+B	3.94	52.9	13.51	261.6

[#] T = tab crack; T+B = the combination of tab crack and bolt bearing failure leading to tearing of beam-end-connector, and T+C = the combination of tab crack and bolt bearing failure leading to tearing of upright wall.

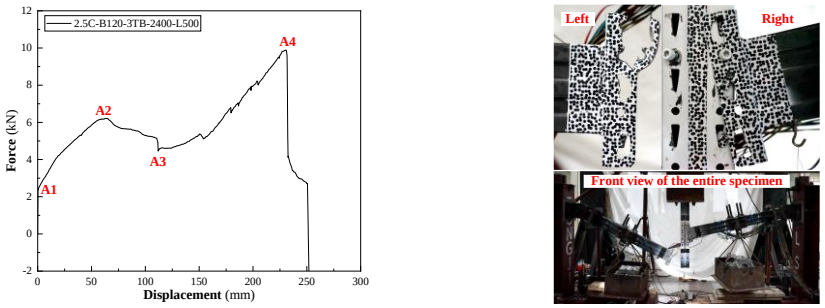

(a) Vertical force-connection displacement curve (b) experimental phenomena

Figure 8: Behaviour of specimen "2.5C-B120-3TB-2400-L500".

3.3 Effects of different parameters on the connection behaviour

From Figure 9, it is evident that increasing the beam height leads to a gradual reduction in the ultimate vertical resistance of the connections and a weakening of the deformation capacity of the connections. Similarly, as the column thickness increases, the ultimate vertical resistance of the connections decreases, and the deformation capacity of the connections diminishes. Notably, for the column thicknesses of 2.0mm and 2.5mm, a change in the failure mode is observed, but the ultimate vertical resistance and deformation capacity show only marginal variations.

When comparing boltless connections with bolted connections, a shift in the failure mode of the connections is observed, and the load-displacement curve exhibits different behaviour. After reaching the first peak point, i.e., the maximum force load-carrying point, the curve descends continuously until the completion of the test, indicating a significant reduction in the ultimate vertical resistance of the connections and a noticeable weakening of the deformation capacity of the connections. In the case of boltless connections, an increase in the number of tabs slightly improves the ultimate load-carrying capacity of the connections and significantly enhances the deformation capacity of the connections.

Additionally, the pallet loads greatly influenced the vertical resistance, and without the pallet loads the vertical resistance and the deformation capacity of the beam-to-upright connections are significantly enhanced. Thus, the pallet loads should be carefully considered in the beam-to-upright substructure of the steel racks structures.

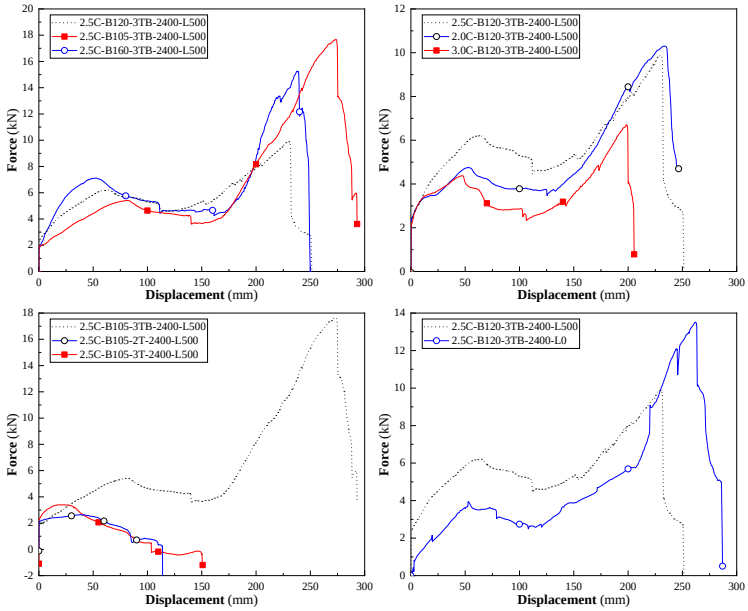

Figure 9: Comparison of different parameters.

3.4 Resistance mechanisms

Using the formulas presented in Section 3.1, the flexural action and the catenary action for enhancing the vertical resistance of the beam-to-upright substructure are calculated. The bending moment and axial force for the specimen 2.5C-B120-3TB-2400-L500 are shown in Figure 10 (a).

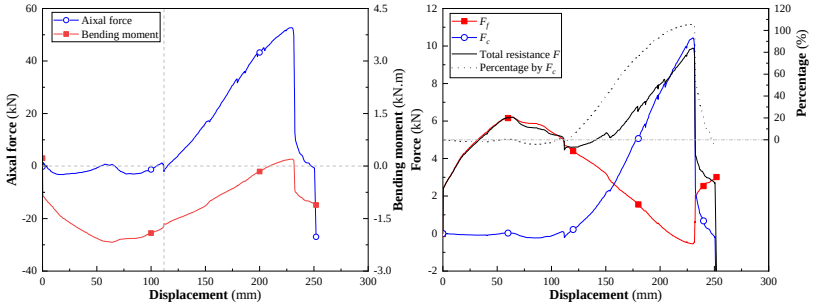

(a) Axial tension force and bending moment (b) Vertical resistance

Figure 10: Axial tension force and bending moment and vertical resistance of specimen “2.5C-B120-3TB-2400-L500”.

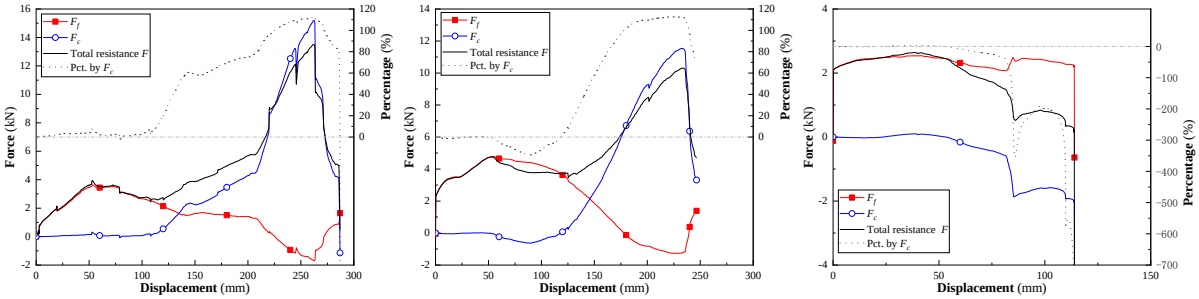

(a) 2.5C-B120-3TB-2400-L0 (b) 2.0C-B120-3TB-2400-L500 (c) 2.5C-B105-2T-2400-L500

Figure 11: Vertical resistance of specimens “2.5C-B120-3TB-2400-L0”, “2.0C-B120-3TB-2400-L500” and “2.5C-B105-2T-2400-L500”.

Figure 10 (b) and Figure 11 indicate the vertical resistance of three failure modes (T, T+B, and T+C) of the beam-to-upright connections under the central column removal scenario.

The vertical resistance of bolted connections follows a consistent trend: the flexural action dominates in the initial loading phase, while the catenary action becomes the main contributor during later loading stages. The presence of pallet loads, beam height, and column thickness has minimal impact on the resistance mechanism development but influences the deformation capacity and ultimate vertical resistance of the connections.

On the other hand, boltless connections exhibit a distinct resistance mechanism from bolted connections. Throughout the loading process, the flexural action predominantly provides vertical resistance against progressive collapse. The catenary action has limited influence during early loading but weakens the vertical resistance of the connections in later stages. The number of tabs has a negligible effect on the resistance mechanism development but significantly affects the deformation capacity and ultimate vertical resistance of the connections.

4 CONCLUSION

This paper investigates the behaviour of steel storage pallet rack beam-to-upright subassemblies under a central column removal scenario. Eight double-half-span substructure tests are conducted considering the influence of connection types, numbers of tabs, pallet loads, column thickness, and beam height. The characteristic failure modes and load-carrying behaviors of the beam-to-upright subassemblies are derived from tests, shedding light on the mechanisms that are resistant to progressive collapse at the beam-to-upright subassemblies. The main conclusions are listed as follows:

(1) The predominant failure modes in cold-formed thin-walled steel storage pallet rack beam-to-upright subassemblies are classified into three categories: tab crack (T), the combination of tab crack and bolt bearing failure leading to tearing of beam-end-connector (T+B), and the combination of tab crack and bolt bearing failure leading to tearing of upright wall (T+C). Notably, the T+C failure mode exclusively occurs in connection substructures featuring a column thickness of 2.0mm.

(2) The vertical resistance of the beam-to-upright connections primarily relies on the interplay between the flexural action and catenary action. In boltless connections, the flexural action maintains dominance throughout the entire loading process, while the catenary action has minimal influence during the early loading stages but weakens the vertical resistance of the beam-to-upright substructures in the later stages of loading. Conversely, for bolted connections, the vertical resistance is initially governed by the flexural action during the early loading stages, gradually transitioning to the catenary action as the primary contributor to vertical resistance in the later stages of loading.

(3) The presence of pallet loads enhances the initial load-carrying capacity of beam-to-upright connections while reducing their ultimate load-carrying capacity and deformation capacity. Increasing the beam height and column thickness results in varying degrees of reduction in the ultimate vertical resistance and deformation capacity of the connections. However, augmenting the number of tabs significantly improves the ultimate load-carrying capacity and deformation capacity of the connections.

(4) Boltless connections exhibit weaker resistance to progressive collapse and are unsuitable for steel pallet rack beam-to-upright subassemblies. Bolted connections are more suitable for steel rack structures. Thus, avoiding the use of boltless connections and prioritizing bolted connections is recommended to enhance the robustness of steel rack structures and improve the resistance to progressive collapse in beam-to-upright subassemblies.

ACKNOWLEDGMENTS

The authors acknowledge support from the National Natural Science Foundation of China (Grant No. 51908347), the Natural Science Foundation of Shanghai (Grant No.22ZR1422700).

REFERENCES

[1] American Society of Civil Engineers, "ASCE 7-05 Minimum Design Loads for Buildings and Other Structures", *Reston*, 2005.

[2] Xianzhong Zhao, Tuo Wang, Yiyi Chen and K. S. Sivakumaran, "Flexural behavior of steel storage rack beam-to-upright connections", *Journal of Constructional Steel Research*, **99**, 161-175, 2014.

[3] Xianzhong Zhao, Liusi Dai and Kim J. R. Rasmussen, "Hysteretic behaviour of steel storage rack beam-to-upright boltless connections", *Journal of Constructional Steel Research*, **144**, 81-105, 2018.

[4] Liusi Dai, Xianzhong Zhao and Kim J. R. Rasmussen, "Cyclic performance of steel storage rack beam-to-upright bolted connections", *Journal of Constructional Steel Research*, **148**, 28-48, 2018.

[5] Liusi Dai, Xianzhong Zhao and Kim J. R. Rasmussen, "Flexural behaviour of steel storage rack beam-to-upright bolted connections", *Thin-Walled Structures*, **124**, 202-217, 2018.

[6] Xianzhong Zhao, Liusi Dai, Tuo Wang, Ken Siva Sivakumaran and Yiyi Chen, "A theoretical model for the rotational stiffness of storage rack beam-to-upright connections", *Journal of Constructional Steel Research*, **133**, 269-281, 2017.

[7] A. L. Y. Ng, R. G. Beale and M. H. R. Godley, "Methods of restraining progressive collapse in rack structures", *Engineering Structures*, **31**(7), 1460-1468, 2009.

[8] Benoit P. Gilbert and Kim J. R. Rasmussen, "Determination of accidental forklift truck impact forces on drive-in steel rack structures", *Engineering Structures*, **33**(5), 1403-1409, 2011.

[9] Benoit P. Gilbert and Kim J. R. Rasmussen, "Impact tests and parametric impact studies on drive-in steel storage racks", *Engineering Structures*, **33**(5), 1410-1422, 2011.

[10] National Technical Committee on Thin-wall Steel Structure Standard, "The specification for design of steel storage racks CECS 23-90", *Beijing: China Association for Engineering Construction Standardization*, 1990.

[11] Shen Yan, Kim J. R. Rasmussen, Xinlu Liu, Liusi Dai and Xianzhong Zhao, "Behaviour of H-section purlin connections in resisting progressive collapse of roofs", *Engineering Structures*, **201**, 2019.

[12] Ling Li, Wei Wang, Yiyi Chen and Yong Lu, "Experimental investigation of beam-to-tubular column moment connections under column removal scenario", *Journal of Constructional Steel Research*, **88**, 244-255, 2013.